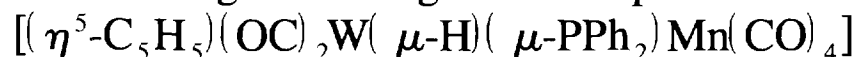


Synthesis, structure and substitution reactions of a heterodimetallic tungsten–manganese complex



Martin J. Mays^{*}, Steven M. Owen, Paul R. Raithby, Paul F. Reinisch, Gregory P. Shields, Gregory A. Solan

University Chemical Laboratory, Lensfield Road, Cambridge CB2 1EW UK

Received 10 May 1996; revised 24 June 1996

Abstract

The room temperature reaction of $[(\eta^5\text{-C}_5\text{H}_5)\text{W}(\text{CO})_3(\text{PPh}_2)]$ with $[\text{Mn}(\text{CO})_5]$ in tetrahydrofuran (THF) followed by protonation with H_3PO_4 gives $[(\eta^5\text{-C}_5\text{H}_5)(\text{OC})_2\text{W}(\mu\text{-H})(\mu\text{-PPh}_2)\text{Mn}(\text{CO})_4]$ **1** as the major product. Among the identified minor products from this reaction are $[\text{Mn}_2(\text{CO})_9(\text{PPh}_2\text{H})]$ **2a**, $[\text{Mn}_2(\text{CO})_9(\text{PPh}_2\text{PPh}_2)]$ **2b**, $[\text{Mn}_2(\mu\text{-H})(\mu\text{-PPh}_2)(\text{CO})_8]$ **2c**, and $[\text{Mn}_2(\mu\text{-PPh}_2)_2(\text{CO})_8]$ **2d**. ^{13}C O reacts with complex **1** substituting both the manganese and tungsten carbonyl groups. In contrast, other two-electron donor ligands, L, only substitute the manganese carbonyl groups to give the substituted products $[(\eta^5\text{-C}_5\text{H}_5)(\text{OC})_2\text{W}(\mu\text{-H})(\mu\text{-PPh}_2)\text{Mn}(\text{CO})_3\text{L}]$ (L = $\text{P}(\text{OMe})_3$ **3a**, PMe_2Ph **3b**, PMePh_2 **3c**, PPh_2H **3d**), $[(\eta^5\text{-C}_5\text{H}_5)(\text{OC})_2\text{W}(\mu\text{-H})(\mu\text{-PPh}_2)\text{Mn}(\text{CO})_2\text{L}_2]$ (L = $\text{P}(\text{OMe})_3$ **4a** or PMe_2Ph **4b**). In the case of the photolytic reaction of **1** with the diphosphine, dppm (dppm = $\text{Ph}_2\text{PCH}_2\text{PPh}_2$), two products are obtained, one in which the ligand is chelated to the manganese centre, $[(\eta^5\text{-C}_5\text{H}_5)(\text{OC})_2\text{W}(\mu\text{-H})(\mu\text{-PPh}_2)\text{Mn}(\text{CO})_2(\text{dppm})]$ **5**, and the other in which the ligand bridges the tungsten manganese centres, $[(\eta^5\text{-C}_5\text{H}_5)(\text{OC})\text{W}(\mu\text{-H})(\mu\text{-PPh}_2)(\mu\text{-dppm})\text{Mn}(\text{CO})_3]$ **6**. Conversion of complex **5** to **6** can be achieved by prolonged UV irradiation of **5**. A single crystal X-ray diffraction study for $[(\eta^5\text{-C}_5\text{H}_5)(\text{OC})_2\text{W}(\mu\text{-H})(\mu\text{-PPh}_2)\text{Mn}(\text{CO})_4]$ **1** is presented.

Keywords: Heterobimetallics; Tungsten; Manganese; Hydrido; Phosphido; Crystal structure

1. Introduction

Studies on the reactivity of heterodinuclear transition metal complexes containing bridging hydride ligands still remain relatively scarce [1,2]. This can be attributed in part to the fact that many such species can only be prepared in low yields.

Homodinuclear transition metal complexes possessing bridging phosphido and hydrido ligands have often been synthesised by the oxidative addition of a secondary phosphine (PR_2H) to an unbridged carbonyl complex [3,4]. As a synthetic strategy for heterodinuclear complexes the preparation of $[(\eta^5\text{-C}_5\text{H}_5)(\text{OC})_2\text{Mo}(\mu\text{-H})(\mu\text{-PPh}_2)\text{Mn}(\text{CO})_4]$ from $[(\eta^5\text{-C}_5\text{H}_5)(\text{OC})_3\text{MoMn}(\text{CO})_5]$ and PPh_2H provides an example of a successful application of the method [5,6]. We have found in our initial studies, however, that photolysis or thermolysis of $[(\eta^5\text{-C}_5\text{H}_5)(\text{OC})_3\text{WMn}(\text{CO})_5]$ with

PPh_2H afforded only trace amounts of the tungsten analogue $[(\eta^5\text{-C}_5\text{H}_5)(\text{OC})_2\text{W}(\mu\text{-H})(\mu\text{-PPh}_2)\text{Mn}(\text{CO})_4]$ **1**.

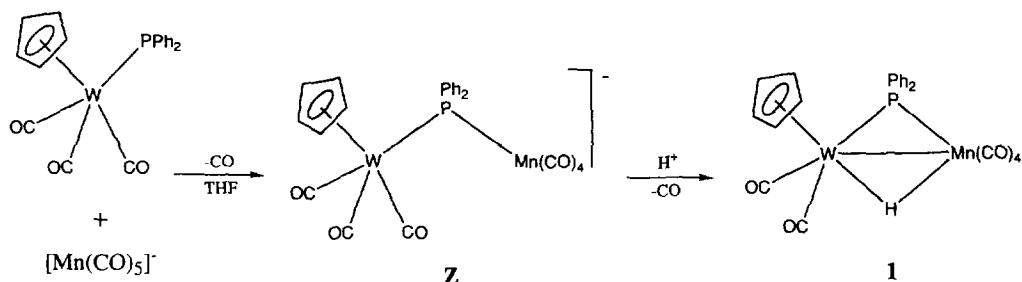
Geoffroy and coworkers have shown that the reaction of $[\text{Mn}(\text{CO})_5\text{H}]$ with $[(\eta^5\text{-C}_5\text{H}_5)\text{Fe}(\text{CO})_2(\text{PPh}_2)]$ gives the complex $[(\eta^5\text{-C}_5\text{H}_5)(\text{OC})\text{Fe}(\mu\text{-H})(\mu\text{-PPh}_2)\text{Mn}(\text{CO})_4]$ in moderate yield [7]. In this paper we report the synthesis of $[(\eta^5\text{-C}_5\text{H}_5)(\text{OC})_2\text{W}(\mu\text{-H})(\mu\text{-PPh}_2)\text{Mn}(\text{CO})_4]$ **1** by a similar route, namely reaction of the anion $[\text{Mn}(\text{CO})_5]^-$ with $[(\eta^5\text{-C}_5\text{H}_5)\text{W}(\text{CO})_3(\text{PPh}_2)]$ followed by protonation with H_3PO_4 (Scheme 1). The fluxional behaviour of **1** and its reactivity towards some two-electron donor ligands have been investigated.

2. Results and discussion

2.1. Preparation of the complex $[(\eta^5\text{-C}_5\text{H}_5)(\text{OC})_2\text{W}(\mu\text{-H})(\mu\text{-PPh}_2)\text{Mn}(\text{CO})_4]$ **1**

The use of a method analogous to that reported for the formation of $[(\eta^5\text{-C}_5\text{H}_5)(\text{OC})_2\text{Mo}(\mu\text{-H})(\mu\text{-PPh}_2)-$

^{*} Corresponding author.



Scheme 1. Synthetic pathway for the preparation of $[(\eta^5\text{-C}_5\text{H}_5)(\text{OC})_2\text{W}(\mu\text{-H})(\mu\text{-PPh}_2)\text{Mn}(\text{CO})_4]$ **1**.

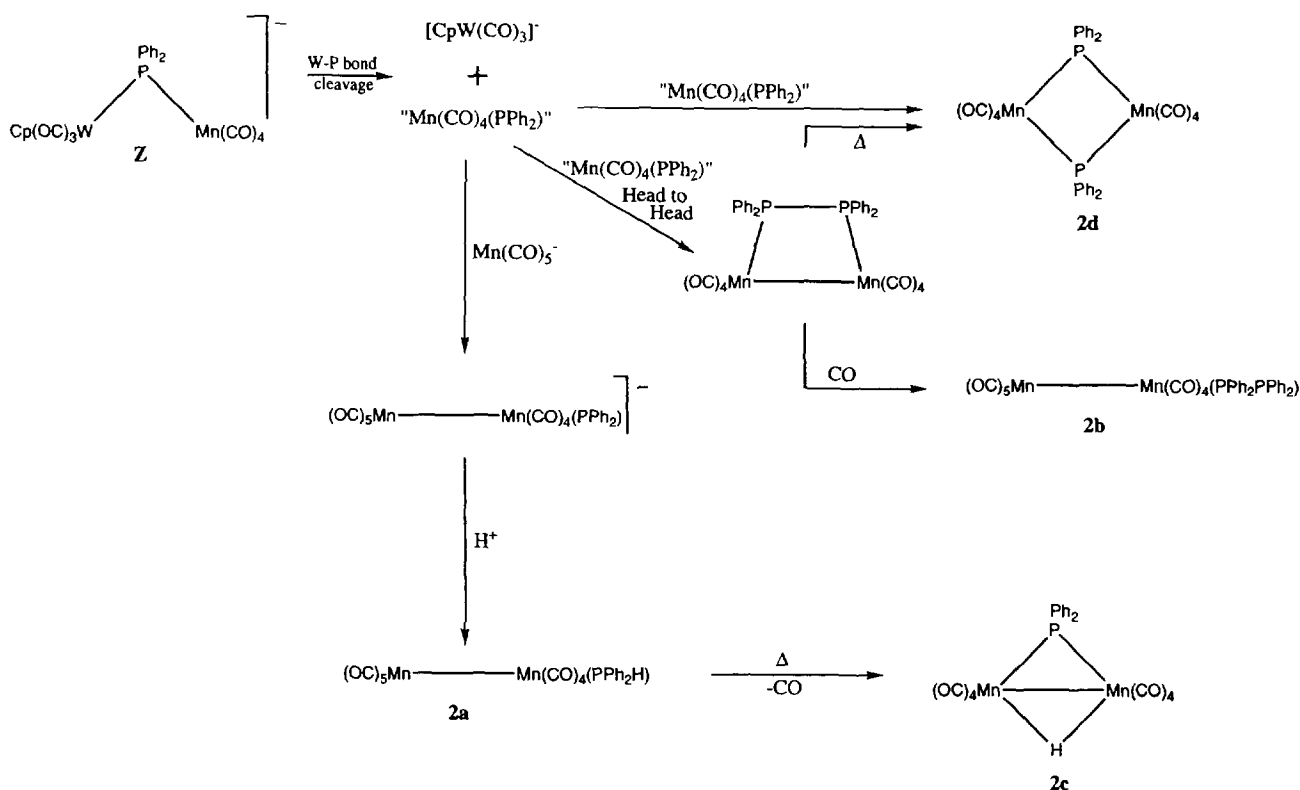
$\text{Mn}(\text{CO})_4$] [5,6], namely the oxidative addition of PPh_2H to $[(\eta^5\text{-C}_5\text{H}_5)(\text{OC})_3\text{WMn}(\text{CO})_5]$ gave $[(\eta^5\text{-C}_5\text{H}_5)(\text{OC})_2\text{W}(\mu\text{-H})(\mu\text{-PPh}_2)\text{Mn}(\text{CO})_4]$ **1** in only very low yield. The room temperature reaction of $[(\eta^5\text{-C}_5\text{H}_5)\text{W}(\text{CO})_3(\text{PPh}_2)]$ [8] with $[\text{Mn}(\text{CO})_5]^-$ [9] followed by protonation with H_3PO_4 , however, afforded a mixture of products with $[(\eta^5\text{-C}_5\text{H}_5)(\text{OC})_2\text{W}(\mu\text{-H})(\mu\text{-PPh}_2)\text{Mn}(\text{CO})_4]$ **1** (ca. 10%) as the major component. Scheme 1 shows the synthetic pathway for the preparation of **1**. The existence of an anionic precursor such as $[(\eta^5\text{-C}_5\text{H}_5)(\text{OC})_2\text{W}(\mu\text{-PPh}_2)\text{Mn}(\text{CO})_4]^-$ **Z** is implied as complex **1** was only isolated upon addition of acid to the reaction mixture. Many of the side-products resulting from this reaction were not characterised owing to their air-sensitive nature, although a number of dimanganese complexes, $[\text{Mn}_2(\text{CO})_9(\text{PPh}_2\text{H})]$ **2a** [10], $[\text{Mn}_2(\text{CO})_9(\text{PPh}_2\text{H})]$ **2b**, $[\text{Mn}_2(\mu\text{-H})(\mu\text{-PPh}_2)(\text{CO})_8]$ **2c** [4,11] and $[\text{Mn}_2(\mu\text{-PPh}_2)_2(\text{CO})_8]$ **2d** [12], were isolated. Both the new complexes **1** and **2b** have been characterised spectroscopically (see Table 1 and Section 4) and, in addition, a single crystal X-ray diffraction study has been performed for **1**.

The variety of products suggests that there are numerous reactions occurring in parallel in the reaction pot. Scheme 2 shows some possible pathways from the proposed anionic precursor complex **Z** which are capable of accounting for the formation of the dimanganese side-products.

The variety of products suggests that there are numerous reactions occurring in parallel in the reaction pot. Scheme 2 shows some possible pathways from the proposed anionic precursor complex **Z** which are capable of accounting for the formation of the dimanganese side-products.

2.1.1. Characterisation and fluxional behaviour of **1**

The isotopic distribution pattern for **1** obtained for the parent molecular ion seen in the electron impact (EI)



Scheme 2. Some possible routes to $[(\eta^5\text{-C}_5\text{H}_5)(\text{OC})_2\text{W}(\mu\text{-H})(\mu\text{-PPh}_2)\text{Mn}(\text{CO})_4]$ **1** and the homodimetallic complexes $[\text{Mn}_2(\text{CO})_9(\text{PPh}_2\text{H})]$ **2a**, $[\text{Mn}_2(\text{CO})_9(\text{P}_2\text{Ph}_4)]$ **2b**, $[\text{Mn}_2(\mu\text{-H})(\mu\text{-PPh}_2)(\text{CO})_8]$ **2c** and $[\text{Mn}_2(\mu\text{-PPh}_2)_2(\text{CO})_8]$ **2d**.

Table 1
IR, ^1H NMR and ^{31}P NMR data for the new complexes

Compound	$\nu(\text{CO}) (\text{cm}^{-1})^a$	^1H NMR (δ) ^b	^{31}P NMR (δ) ^c
1	2072m, 2001m, 1977s, 1961s 1890m	7.4–7.2 (m, 10H, <i>Ph</i>), 5.12 (s, 5H, <i>Cp</i>), –15.35 (d, $^2J(\text{PH})$ 27.3, $^1J(\text{WH})$ 41.9, 1H, $\mu\text{-H}$)	–21.2 (s, $^1J(\text{WP})$ 226.8, $\mu\text{-PPh}_2$)
2b	2090w, 2011w, 1996s, 1973w, 1940w	7.8–6.9 (m, 20H, <i>Ph</i>)	–76.2 (d, $^1J(\text{PP})$ 350.7, Mn-PPh_2), –144.6 (d, $\text{Mn-PPh}_2\text{PPh}_2$)
3a	2033m, 1956s, 1952sh, 1933s, 1873s	8.0–6.9 (m, 10H, <i>Ph</i>), 5.08 (s, 5H, <i>Cp</i>), 3.82 (d, $^3J(\text{PH})$ 11.5, 9H, <i>OMe</i>), –15.8 (dd, $^2J(\text{PH})$ 27.0, 27.0, $^1J(\text{WH})$ 44.4, 1H, $\mu\text{-H}$)	–15.2 (s, $\mu\text{-PPh}_2$), 47.3 (s, br, $\text{P}(\text{OMe})_3$)
3b	2020w, 1947s, 1934s, 1916s, 1871s	7.9–6.9 (m, 15H, <i>Ph</i>), 4.66 (s, 5H, <i>Cp</i>), 2.04 (d, $^2J(\text{PH})$ 8.0, 6H, PMe_2Ph), –15.98 (dd, $^2J(\text{PH})$ 25.5, 25.5, $^1J(\text{WH})$ 46.7, 1H, $\mu\text{-H}$)	–11.47 (s, $\mu\text{-PPh}_2$), –107.6 (s, PMe_2Ph)
3c	2022w, 1946s, 1936s, 1918m, 1871m	8.0–6.9 (m, 20H, <i>Ph</i>), 4.63 (s, 5H, <i>Cp</i>), 2.29 (d, $^2J(\text{PH})$ 7.5, 3H, PMePh_2), –15.90 (dd, $^2J(\text{PH})$ 28.0, 22.5, 1H, $\mu\text{-H}$)	–9.6 (s, $\mu\text{-PPh}_2$), –92.9 (s, PMePh_2)
3d	2026w, 1949s, 1940s, 1923m, 1874m	Major (95%): 7.9–6.9 (m, 20H, <i>Ph</i>), 5.79 (d, $^1J(\text{PH})$ 334.5, 1H, PPh_2H), 4.64 (s, 5H, <i>Cp</i>), –15.82 (dd, $^2J(\text{PH})$ 26.2, 26.2, 1H, $\mu\text{-H}$). Minor (5%): 4.62 (<i>Cp</i>)	Major (95%): –8.7 (s, $\mu\text{-PPh}_2$), –94.5 (s, PPh_2H), Minor (5%): 4.3 (d, $^2J(\text{PP})$ 61.0, $\mu\text{-PPh}_2$), –115.5 (d, PPh_2H)
4a	1994w, 1939s, 1908s, 1859s	8.0–6.9 (m, 10H, <i>Ph</i>), 4.97 (s, 5H, <i>Cp</i>), 3.82 (d, $^3J(\text{PH})$ 11.0, 9H, <i>OMe</i>), 3.39 (d, $^3J(\text{PH})$ 10.9, 9H, <i>OMe</i>), –16.55 (ddd, $^2J(\text{PH})$ 32.4, 26.7, 14.7, 1H, $\mu\text{-H}$)	51.3 (m, $\text{P}(\text{OMe})_3$), 47.2 (m, $\text{P}(\text{OMe})_3$), –17.0 (d, $^2J(\text{PP})$ 30.8, $\mu\text{-PPh}_2$)
4b	1963w, 1931s, 1873s, 1853m	8.1–6.9 (m, 20H, <i>Ph</i>), 4.45 (s, 5H, <i>Cp</i>), 1.70 (s, br, 6H, PMe_2Ph), 1.56 (d, $^2J(\text{PH})$ 6.4, 6H, PMe_2Ph), –17.70 (ddd, $^2J(\text{PH})$ 29.7, 29.7, 14.7, 1H, $\mu\text{-H}$)	–16.6 (s, $\mu\text{-PPh}_2$), –102.1 (s, PMe_2Ph), –102.5 (s, PMe_2Ph)
5	1945sh, 1923s, 1871m, 1853m	8.1–6.5 (m, 30H, <i>Ph</i>), 4.80 (s, 5H, <i>Cp</i>), 4.55 (m, 2H, CH_2), –12.50 (ddd, $^2J(\text{PH})$ 36.6, 19.5, 15.1, 1H, $\mu\text{-H}$)	–7.5 (m, $\mu\text{-PPh}_2$), –101.1 (d, $^2J(\text{PP})_{\text{dppm}}$) 37.9, dppm(<i>cis</i> $\mu\text{-P}$), –129.6 (dd, $^2J(\text{P}_\mu\text{-P}_{\text{trans}})$) 39.3, dppm(<i>trans</i> $\mu\text{-P}$) ^d
6	1938s, 1934sh, 1873s	7.9–6.9 (m, 30H, <i>Ph</i>), 4.77 (s, 5H, <i>Cp</i>), 4.25 (m, 1H, CH_2), 3.40 (m, 1H, CH_2), –11.30 (ddd, $^2J(\text{PH})$ 40.1, 1H, $\mu\text{-H}$)	–51.6 (m, $^1J(\text{WP})$ 171.4, $\mu\text{-PPh}_2$), –61.2 (dd, 40.1, 16.2, $^2J(\text{PP})_{\text{dppm}}$ 133.4, $^2J(\text{P}_\mu\text{-P}_{\text{trans}})$ 24.2, dppm(<i>trans</i> $\mu\text{-P}$)), –112.5 (d, $^1J(\text{WP})$ 178.5, dppm(<i>cis</i> $\mu\text{-P}$) ^d)

^a Recorded in *n*-hexane solution.

^b ^1H chemical shifts (δ ppm) relative to SiMe_4 (0.0 ppm), coupling constants (*J* Hz) in CDCl_3 at 293 K.

^c ^{31}P chemical shifts (δ ppm) relative to external $\text{P}(\text{OMe})_3$ (0.0 ppm) (upfield shifts negative), $\{^1\text{H}\}$ -gated decoupled, measured in CDCl_3 at 293 K.

^d Recorded at 250 K.

mass spectrum is indicative of a W–Mn species. The peak of maximum intensity in the molecular ion multiplet ($M^+ = 658$) corresponds to $^{184}\text{W}^{55}\text{Mn}$ and there are fragment ions due to the loss of $n\text{CO}$ ($n = 1-4$). The IR spectrum of **1** in hexane shows five carbonyl absorption bands, the two bands of lower frequency being attributed to tungsten carbonyls by comparison with $[(\eta^5\text{-C}_5\text{H}_5)_2\text{W}_2(\mu\text{-H})(\mu\text{-PPh}_2)(\text{CO})_4]$ [13] and the three at higher frequency to manganese carbonyls by analogy with $[\text{Mn}_2(\mu\text{-H})(\mu\text{-PPh}_2)(\text{CO})_8]$ [11].

The ^1H NMR spectrum of **1** at 293 K shows broad resonances in the phenyl region and a sharp singlet due to the cyclopentadienyl ligand. In addition, a doublet (with ^{183}W satellites) is seen in the hydride region ($\delta - 15.35$ $^2J(\text{PH})$ 27.3, $^1J(\text{WH})$ 41.9 Hz). The values of the coupling constants $^2J(\text{PH})$ and $^1J(\text{WH})$ are within the range reported for related complexes [2,14,15]. The $^{31}\text{P}\{-^1\text{H}\}$ NMR spectrum for **1** consists of one peak at $\delta - 21.2$ (relative to $\text{P}(\text{OMe})_3$ (0.0 ppm)), slightly broadened due to the ^{55}Mn quadrupolar nucleus, with ^{183}W satellites ($^1J(\text{WP})$ 226.8 Hz).

The $^{13}\text{C}\{-^1\text{H}\}$ NMR spectrum of an unenriched sample of **1** at 293 K (Fig. 1(a)) reveals only three resonances (δ 217.8, 216.5, 210.0) in the carbonyl region, corresponding to the manganese carbonyls alone. The downfield tungsten carbonyl signals are very broad in this spectrum at this temperature but can be identified when **1** is enriched with ^{13}CO (see Fig. 1(b) and below).

In the phenyl region peaks due to the *ipso*-, *ortho*-, *para*- and *meta*-carbon atoms of the two equivalent phenyl groups are visible at 293 K. When the spectrum of **1** is recorded at 225 K (Fig. 1(c)) well defined resonances for all six terminal carbonyl groups are observed, and the peaks due to the tungsten carbonyls can be assigned on the basis of the similarity in chemical shifts to those of the CO groups in $[(\eta^5\text{-C}_5\text{H}_5)(\text{OC})_2\text{W}(\mu\text{-PPh}_2)\text{Mo}(\text{CO})_5]$ [16]. The carbonyl resonance most downfield is a sharp doublet ($^2J(\text{PC})$ 20.7 Hz) and is thus assigned to the W–CO cisoid to the phosphido bridge [17]. The singlet resonance immediately upfield of this doublet is identified as due to the other W–CO, transoid to the phosphido bridge. All four manganese carbonyl resonances are resolved at 225 K and are upfield of the tungsten carbonyl peaks, all exhibiting characteristic quadrupolar broadening. At this temperature, the phenyl resonances become inequivalent and two sets of doublets are seen for the P-C_{ipso} and *ortho*-Ph carbon atoms of the two phenyl groups. One *para*-Ph resonance is seen as a singlet, the other being obscured by one of the *meta*-Ph resonances. The final *meta*-Ph resonance is seen as a doublet.

Similar variable-temperature ^{13}C NMR spectra have been observed previously for $[(\eta^5\text{-C}_5\text{H}_5)(\text{OC})_2\text{Mo}(\mu\text{-AsMe})_2\text{Fe}(\text{CO})_4]$ [18], $[(\eta^5\text{-C}_5\text{H}_5)_2\text{Mo}_2(\mu\text{-H})(\mu\text{-PPhR})(\text{CO})_4]$ [19] and $[(\eta^5\text{-C}_5\text{H}_5)(\text{OC})_2\text{Mo}(\mu\text{-H})(\mu\text{-PPh}_2)\text{Mn}(\text{CO})_4]$ [5,6]. In these cases a fluxional process

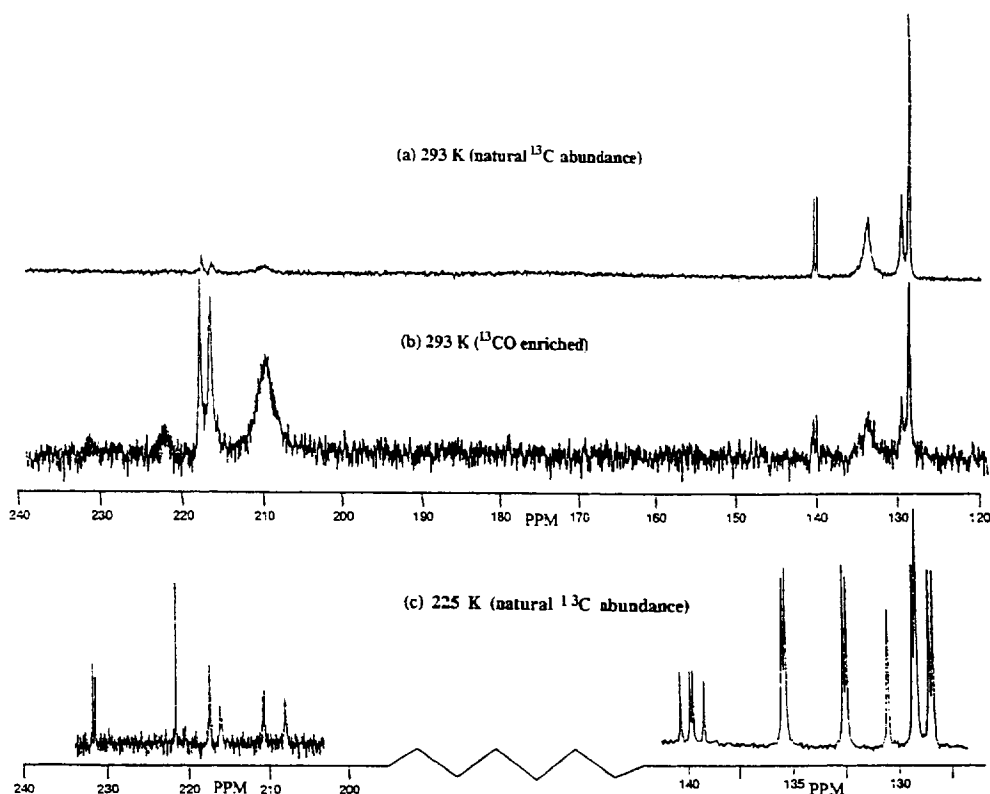
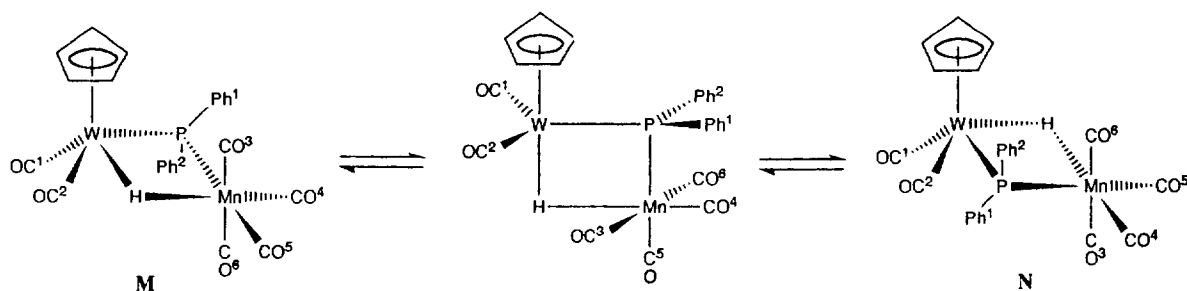


Fig. 1. $^{13}\text{C}\{-^1\text{H}\}$ NMR spectra for samples of **1** in CDCl_3 recorded at (a) 293 K (natural abundance), (b) 293 K (^{13}CO enriched) and (c) 225 K. Only the carbonyl and phenyl regions are shown.



Scheme 3. Proposed fluxional process to explain the temperature variation of the ^{13}C NMR spectra of complex $[(\eta^5\text{-C}_5\text{H}_5)(\text{OC})_2\text{W}(\mu\text{-H})(\mu\text{-PPh}_2)\text{Mn}(\text{CO})_4]$ **1**.

involving a change in geometry around the Group 6 metal centre from square pyramidal to trigonal bipyramidal and back to square pyramidal has been postulated to account for the merging at higher temperatures of the signals for the tungsten carbonyls, two of the manganese carbonyls and the phenyl groups. In **1** a similar process is envisaged, in which enantiomer **M** is converted to enantiomer **N** with consequent interconversion of CO^1/CO^2 , CO^6/CO^3 and Ph^1/Ph^2 (Scheme 3). Although complete coalescence of the tungsten carbonyls was not observed at 293 K, the broadness of the signals is consistent with the onset of rapid interconversion.

The molecular structure of complex $[(\eta^5\text{-C}_5\text{H}_5)(\text{OC})_2\text{W}(\mu\text{-H})(\mu\text{-PPh}_2)\text{Mn}(\text{CO})_4]$ **1** has been determined by a single crystal X-ray diffraction study. The structure is depicted in Fig. 2; Table 2 lists selected bond distances and angles, and atomic coordinates are given in Table 3.

The coordination of the ligands around the W and Mn is approximately square pyramidal and octahedral

respectively, and is essentially identical to that in the related complex $[(\eta^5\text{-C}_5\text{H}_5)(\text{OC})_2\text{Mo}(\mu\text{-H})(\mu\text{-PPh}_2)\text{Mn}(\text{CO})_4]$ [2]. Although the bridging hydride was not located, it is thought to lie in the WMnP plane on the opposite side of the W-Mn vector from the phosphido bridge, as in the homometallic complexes, $[\text{Mn}_2(\mu\text{-H})(\mu\text{-PPh}_2)(\text{CO})_8]$ [4,11] and $[(\eta^5\text{-C}_5\text{H}_5)_2\text{Mo}_2(\mu\text{-H})(\mu\text{-PMe}_2)(\text{CO})_4]$ [20].

The W-Mn bond distance ($3.087(3)\text{Å}$) is slightly shorter than the W-Mn bond length (3.16Å) in the unbridged complex $[(\eta^5\text{-C}_5\text{H}_5)(\text{OC})_3\text{WMn}(\text{CO})_5]$ [21] but longer than two other known W-Mn distances of $2.9939(8)$ and $2.696(1)\text{Å}$ in $[(\text{OC})_4\text{W}\{\mu\text{-C}(\text{CO}_2\text{-Me})\}\text{Mn}(\text{CO})_2(\eta^5\text{-C}_5\text{H}_5)]$ [22] and $[(\eta^5\text{-C}_5\text{H}_5)(\text{OC})_3\text{W}\{\mu\text{-C}(p\text{-tol})\text{C}(\text{O})\text{Me}\}\text{Mn}(\text{CO})_3]$ [23] respectively. The tungsten-phosphorus distance ($2.419(3)\text{Å}$) in **1** is slightly shorter than the corresponding value ($2.435(1)\text{Å}$) for the molybdenum-phosphorus distance in $[(\eta^5\text{-C}_5\text{H}_5)(\text{OC})_2\text{Mo}(\mu\text{-H})(\mu\text{-PPh}_2)\text{Mn}(\text{CO})_4]$ [2]. The remaining structural parameters do not deviate significantly from those in the MnMo analogue [2].

2.1.2. Characterisation of $[\text{Mn}_2(\text{CO})_9(\text{PPh}_2\text{PPh}_2)]$ **2b**

The EI mass spectrum of **2b** shows parent peaks at 676 (the molecular ion peak being calculated as 732)

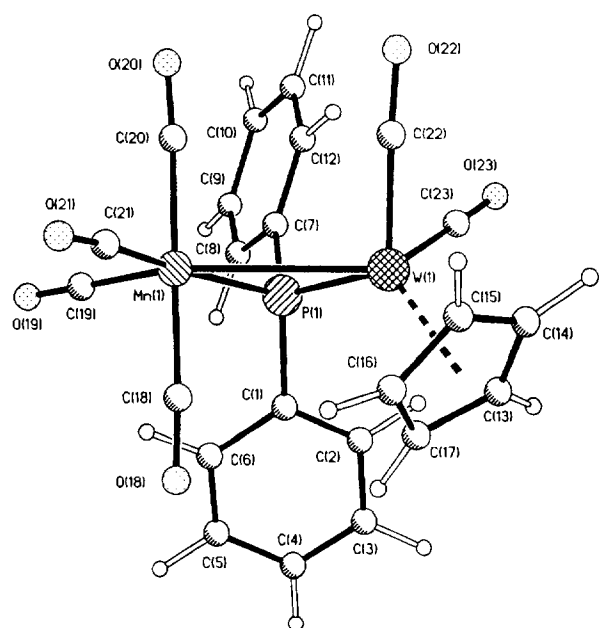


Fig. 2. Molecular structure of $[(\eta^5\text{-C}_5\text{H}_5)(\text{OC})_2\text{W}(\mu\text{-H})(\mu\text{-PPh}_2)\text{Mn}(\text{CO})_4]$ **1** including the atom numbering scheme.

Table 2
Selected bond lengths (Å) and angles (deg) for $[(\eta^5\text{-C}_5\text{H}_5)(\text{OC})_2\text{W}(\mu\text{-H})(\mu\text{-PPh}_2)\text{Mn}(\text{CO})_4]$ **1**

Bond distance			
Mn(1)–W(1)	3.087(3)	P(1)–C(7)	1.813(16)
Mn(1)–C(20)	1.895(24)	P(1)–C(1)	1.857(17)
Mn(1)–C(21)	1.831(22)	Mn(1)–C(19)	1.786(18)
Mn(1)–C(18)	1.840(21)	Mn(1)–P(1)	2.286(5)
W(1)–C(22)	1.913(17)	W(1)–C(23)	1.963(19)
W(1)–P(1)	2.419(3)	W(1)–C(13)	2.293(16)
W(1)–C(14)	2.290(17)	W(1)–C(15)	2.328(17)
W(1)–C(16)	2.408(21)	W(1)–C(17)	2.369(21)
Bond angle			
Mn(1)–P(1)–W(1)	82.0(1)	C(23)–W(1)–P(1)	80.7(5)
P(1)–W(1)–Mn(1)	47.2(1)	C(1)–P(1)–W(1)	116.8(5)
C(1)–P(1)–C(7)	101.5(7)	C(7)–P(1)–Mn(1)	116.0(6)
P(1)–Mn(1)–W(1)	50.9(1)		
	range O–C–Mn(1)		174.8(22)–177.2(19)
	range O–C–W(1)		177.4(14)–177.5(15)

Table 3
Atomic coordinates for complex $[(\eta^5\text{-C}_5\text{H}_5)(\text{OC})_2\text{W}(\mu\text{-H})(\mu\text{-PPh}_2)\text{Mn}(\text{CO})_4] \mathbf{1}$

	x	y	z
W1	0.2160	0.1221	0.3279
	0.0000	0.0000	0.0000
Mn1	0.1203	0.2423	0.2923
	0.0001	0.0002	0.0002
P1	0.1417	0.1334	0.1925
	0.0001	0.0003	0.0003
C1	0.1026	0.0259	0.1620
	0.0006	0.0012	0.0010
C2	0.1247	-0.0562	0.1519
	0.0007	0.0012	0.0011
H2	0.1643	-0.0578	0.1597
	0.0007	0.0012	0.0011
C3	0.0967	-0.1409	0.1311
	0.0008	0.0012	0.0013
H3	0.1153	-0.2069	0.1267
	0.0008	0.0012	0.0013
C4	0.0466	-0.1385	0.1168
	0.0007	0.0012	0.0014
H4	0.0246	-0.2017	0.0969
	0.0007	0.0012	0.0014
C5	0.0240	-0.0537	0.1281
	0.0006	0.0013	0.0013
H5	-0.0158	-0.0520	0.1183
	0.0006	0.0013	0.0013
C6	0.0509	0.0275	0.1514
	0.0005	0.0012	0.0012
H6	0.0326	0.0923	0.1616
	0.0005	0.0012	0.0012
C7	0.1421	0.1748	0.0723
	0.0006	0.0012	0.0010
C8	0.1021	0.1567	-0.1012
	0.0006	0.0012	0.0011
H8	0.0716	0.1135	-0.0019
	0.0006	0.0012	0.0011
C9	0.1003	0.1913	-0.0996
	0.0008	0.0016	0.0013
H9	0.0696	0.1734	-0.1618
	0.0008	0.0016	0.0013
C10	0.1404	0.2531	-0.1114
	0.0007	0.0015	0.0012
H10	0.1387	0.2841	-0.1814
	0.0007	0.0015	0.0012
C11	0.1807	0.2713	-0.0310
	0.0007	0.0015	0.0014
H11	0.2114	0.3144	-0.0383
	0.0007	0.0015	0.0014
C12	0.1808	0.2328	0.0594
	0.0006	0.0013	0.0012
H12	0.2117	0.2483	0.1219
	0.0006	0.0013	0.0012
C13	0.2343	-0.0302	0.3790
	0.0008	0.0012	0.0012
H13	0.2382	-0.0819	0.3258
	0.0008	0.0012	0.0012
C14	0.2722	0.0269	0.4331
	0.0007	0.0014	0.0012
H14	0.3106	0.0250	0.4304
	0.0007	0.0014	0.0012
C15	0.2535	0.0864	0.4909
	0.0008	0.0015	0.0013
H15	0.2738	0.1416	0.5372
	0.0003	0.0015	0.0013

Table 3 (continued)

	x	y	z
C16	0.2052	0.0633	0.4794
	0.0008	0.0017	0.0013
H16	0.1810	0.0938	0.5189
	0.0008	0.0017	0.0013
C17	0.1909	-0.0105	0.4040
	0.0008	0.0014	0.0013
H17	0.1546	-0.0420	0.3749
	0.0008	0.0014	0.0013
C18	0.0936	0.1468	0.3494
	0.0007	0.0014	0.0013
C19	0.0603	0.2690	0.2130
	0.0007	0.0013	0.0014
C20	0.1503	0.3426	0.2409
	0.0009	0.0015	0.0016
C21	0.1174	0.3197	0.3934
	0.0007	0.0017	0.0014
C22	0.2558	0.2314	0.3257
	0.0006	0.0012	0.0012
C23	0.2453	0.0942	0.2204
	0.0007	0.0011	0.0012
O18	0.0755	0.0892	0.3869
	0.0006	0.0011	0.0010
O19	0.0228	0.2841	0.1580
	0.0006	0.0012	0.0012
O20	0.1660	0.4045	0.2122
	0.0007	0.0012	0.0013
O21	0.1139	0.3623	0.4589
	0.0008	0.0014	0.0014
O22	0.2821	0.2970	0.3251
	0.0005	0.0010	0.0012
O23	0.2642	0.0793	0.1594
	0.0005	0.0010	0.0009

which corresponds to a structure which has two carbonyls less than the proposed parent compound.

In the $^{31}\text{P}\{-^1\text{H}\}$ NMR spectrum of **2b**, doublets are observed at $\delta -76.2$ ($^1J(\text{PP})$ 305.7 Hz) and $\delta -144.6$. A coupling constant of 305.7 Hz is indicative of a directly bonded phosphorus–phosphorus coupling [24]. Five bands are seen in the ν_{CO} (hexane) region of the IR spectrum of **2b**, which is consistent with the presence of an axially substituted P_2Ph_4 group [25]. Such axial substitution is not unexpected in view of the steric bulk of the P_2Ph_4 group.

2.2. Reactions of $[(\eta^5\text{-C}_5\text{H}_5)(\text{OC})_2\text{W}(\mu\text{-H})(\mu\text{-PPh}_2)\text{Mn}(\text{CO})_4] \mathbf{1}$ with phosphines, phosphite and ^{13}CO

In order to ascertain whether **1** reacts with two-electron donor ligands in a site-selective manner, and whether it forms addition or substitution products, studies were carried out of its reactions with ^{13}CO , $\text{P}(\text{OMe})_3$ and a variety of phosphines (PMe_2Ph , PMePh_2 , PPh_2H and the diphosphine, dppm).

2.2.1. Reaction of **1** with ^{13}CO

A solution of **1** in toluene was stirred under an atmosphere of ^{13}CO at 333 K for 48 h. The mass spec-

trum, ^1H , $^{31}\text{P}\{-^1\text{H}\}$ and $^{13}\text{C}\{-^1\text{H}\}$ NMR spectra of the product are consistent with **1** having undergone a substitution reaction with ^{13}CO under these conditions. A comparison of the $^{13}\text{C}\{-^1\text{H}\}$ NMR spectra at 293 K for a sample of **1** containing ^{13}CO in natural abundance with that for a ^{13}CO -labelled sample indicates that substitution of the CO groups on both the manganese and tungsten atoms has taken place (Fig. 1(a) and Fig. 1(b)). The reaction of CO with the related phosphido-bridged complex $[(\eta^5\text{-C}_5\text{H}_5)(\text{OC})_2\text{W}(\mu\text{-PPh}_2)\text{Mo}(\text{CO})_5]$ gives the addition product $[(\eta^5\text{-C}_5\text{H}_5)(\text{OC})_3\text{W}(\mu\text{-PPh}_2)\text{Mo}(\text{CO})_5]$ in which a metal–metal bond has been cleaved [16], but in the reaction of CO with complex **1** the metal–metal interaction is maintained.

2.2.2. Reaction of **1** with $\text{P}(\text{OMe})_3$, PMe_2Ph , PMePh_2 and dppm

The reaction of **1** under UV irradiation in toluene–hexane solutions with $\text{P}(\text{OMe})_3$, PMe_2Ph , PMePh_2 and dppm , and under thermolysis in toluene with PPh_2H , affords substitution products of general formula $[(\eta^5\text{-C}_5\text{H}_5)(\text{OC})_2\text{W}(\mu\text{-H})(\mu\text{-PPh}_2)\text{Mn}(\text{CO})_3\text{L}]$ ($\text{L} = \text{P}(\text{OMe})_3$ **3a**, PMe_2Ph **3b**, PMePh_2 **3c**, PPh_2H **3d**), $[(\eta^5\text{-C}_5\text{H}_5)(\text{OC})_2\text{W}(\mu\text{-H})(\mu\text{-PPh}_2)\text{Mn}(\text{CO})_2\text{L}_2]$ ($\text{L} = \text{P}(\text{OMe})_3$ **4a**, PMe_2Ph **4b**; $\text{L}_2 = \text{dppm-PP}'$ **5**) and $[(\eta^5\text{-C}_5\text{H}_5)(\text{OC})\text{W}(\mu\text{-H})(\mu\text{-PPh}_2)(\mu\text{-dppm})\text{Mn}(\text{CO})_3]$ **6**. All the complexes **3–6** have been characterised on the

basis of mass spectrometry, micro-analysis, IR and ^1H and ^{31}P NMR spectroscopy (see Table 1 and Section 4). In addition, some of the complexes have been characterised by ^{13}C NMR spectroscopy (see Table 1 and Section 4).

The ν_{CO} (hexane) region of the IR spectra of complexes **3b–d** show five absorptions, while that for **3a** shows four absorptions and a shoulder, consistent in each case with mono-substitution having taken place. In the case of **3a** a $^{13}\text{C}\{-^1\text{H}\}$ NMR spectrum recorded at 240 K shows two sharp downfield resonances (δ 233.3, 224.9) assigned to the W–CO groups on the basis of a lack of quadrupolar broadening. The remaining three higher field ^{13}C resonances (δ 220.8, 213.5, 208.5) are ^{55}Mn quadrupole broadened and are assigned to the three Mn–CO groups.

The ^1H NMR spectra of **3a–d** show the bridging hydride to be coupled to the two phosphorus nuclei, with $^2J(\text{PH})$ values ranging from 22.5–27.0 Hz. In some cases ^{183}W satellites are also observed. The $^2J(\text{PH})$ values are indicative of the hydride being cis to both the phosphido bridge and to the terminal phosphorus ligand, since the value of a cis $^2J(\text{PH})$ coupling across a manganese centre is usually between 20 and 50 Hz, whereas that of a trans $^2J(\text{PH})$ is generally around 150 Hz [26].

The $^{31}\text{P}\{-^1\text{H}\}$ NMR data for complexes **3a–c** indicate

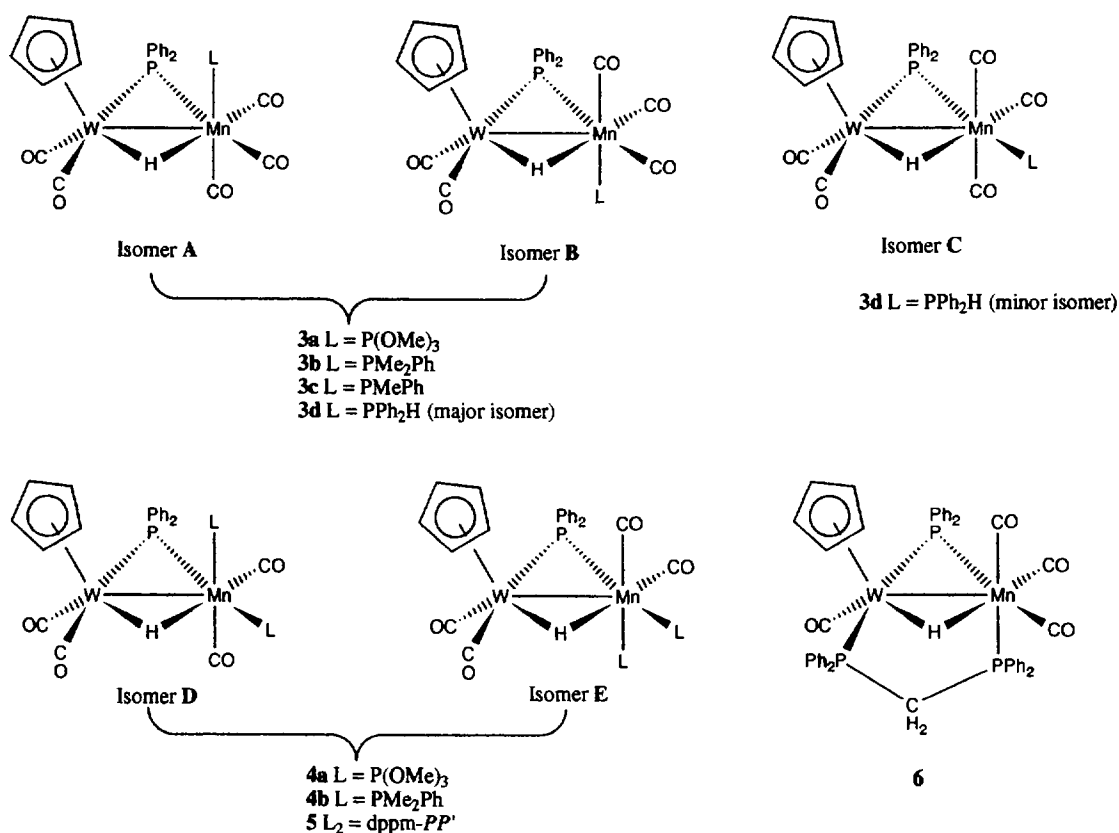


Fig. 3. Proposed structures for the substituted derivatives **3**, **4**, **5** and **6** of $[(\eta^5\text{-C}_5\text{H}_5)(\text{OC})_2\text{W}(\mu\text{-H})(\mu\text{-PPh}_2)\text{Mn}(\text{CO})_4]$ **1**.

the presence of only one isomer, whereas for **3d** two isomers are present in a ratio of 95:5. There are no resolved phosphorus–phosphorus couplings for **3a–c** or for the major isomer of **3d**. However, the minor isomer of **3d** clearly shows such a coupling ($^2J(\text{PP})$ 61.0 Hz). This suggests that the phosphido bridge and the terminal phosphine ligands are positioned mutually trans in the minor isomer of **3d** but cis in all other cases. There are then two possible geometries, **A** and **B** (Fig. 3), for complexes **3a–c** and **3d** (major isomer). Although the data do not permit a distinction to be made between these geometries, the steric restrictions imposed by the cyclopentadienyl group would be minimised in the case of **B**. Structure **C** (Fig. 3) is suggested for **3d** (minor isomer) as this is the only possible structure with the phosphine group cis to the bridging hydride and trans to the bridging phosphido group.

The IR spectra of complexes **4a**, **4b** and **5** are consistent with disubstitution having occurred, with four absorptions being seen in the ν_{CO} (hexane) region for **4a** and **4b** and three absorptions and a shoulder for **5**. The carbonyl regions of the $^{13}\text{C}\{-^1\text{H}\}$ NMR spectra of complexes **4a** and **5** confirm that disubstitution has taken place and, in addition, indicate that it has occurred specifically at the manganese centre. Two downfield resonances in each spectrum can be assigned to the tungsten carbonyl groups, both on account of their relatively sharp nature and by comparison of their chemical shifts with those for the corresponding CO resonances in the $^{13}\text{C}\{-^1\text{H}\}$ NMR spectra of complexes **1** and **3a**. The remaining two higher field resonances for **4a** and **5**, attributed to the manganese carbonyl groups, are significantly broadened, presumably due to the ^{55}Mn quadrupole, and possibly also to unresolved coupling to the phosphorus nuclei.

In the ^1H NMR spectra of **4a**, **4b** and **5** the hydride resonances are coupled to three phosphorus nuclei in each case, the magnitude of $^2J(\text{PH})$ (14.7–36.6 Hz) being indicative of the bridging hydride occupying a position cis to all three phosphorus nuclei.

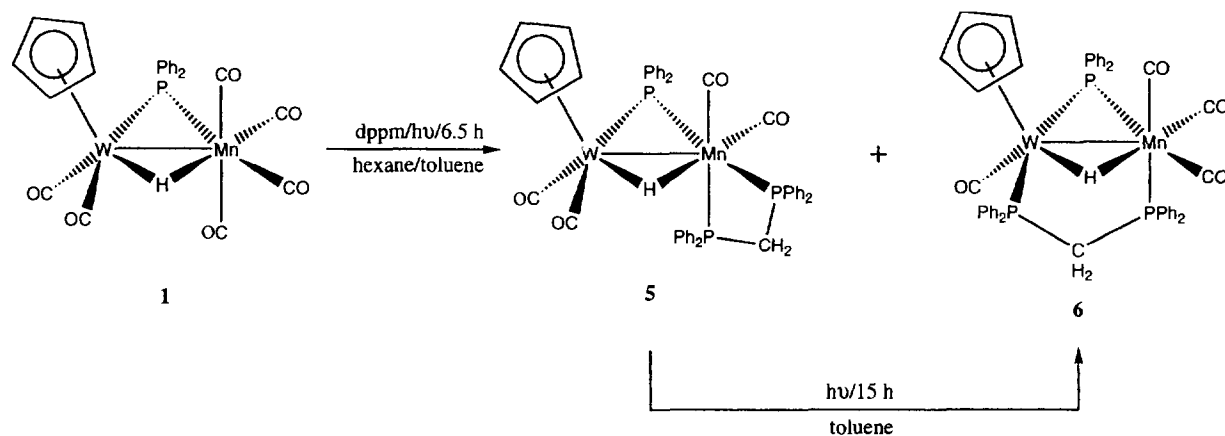
The $^{31}\text{P}\{-^1\text{H}\}$ NMR spectrum of **4a** shows a doublet signal ($^2J(\text{PP})$ 30.8 Hz) due to the $\mu\text{-PPh}_2$ moiety, but the two $\text{P}(\text{OMe})_3$ signals are both too broad to allow resolution of coupling. Complex **5** has three signals in its $^{31}\text{P}\{-^1\text{H}\}$ NMR spectrum recorded at 250 K. The downfield signal at $\delta - 7.5$ is assigned to the phosphido bridge, and the higher field signals at $\delta - 101.1$ (d, $^2J(\text{PP})$ 37.9 Hz) and $\delta - 129.6$ (t, $^2J(\text{PP})$ 37.9, 39.3 Hz) are assigned respectively to the dppm resonances cis and trans to the phosphido bridge. A $^2J(\text{PP})_{\text{dppm}}$ of 37.9 Hz is a reasonable value for the coupling between two phosphorus atoms of a dppm moiety chelating to a manganese centre [27].

Two possible structures, **D** and **E**, in which one phosphorus moiety is cis and the other trans to the phosphido group and in which both are cis to the bridging hydride, can be drawn for the disubstituted complexes **4a**, **4b** and **5** (Fig. 3). A crystal structure of the analogous compound $[(\eta^5\text{-C}_5\text{H}_5)(\text{OC})_2\text{Mo}(\mu\text{-H})(\mu\text{-PPh}_2)\text{Mn}(\text{CO})_2(\text{dppm})]$ shows that this complex adopts a structure of type **E**, this conformation minimising the potential interaction between the cyclopentadienyl moiety and the substituted ligands [5,6]. A similar structure is thus proposed for **4a**, **4b** and **5**.

The UV irradiation of **1** with dppm gives, in addition to **5**, the bridged dppm complex $[(\eta^5\text{-C}_5\text{H}_5)(\text{OC})\text{W}(\mu\text{-H})(\mu\text{-PPh}_2)(\mu\text{-dppm})\text{Mn}(\text{CO})_3]$ **6**. Alternatively, complex **6** can be formed in low yield by prolonged UV irradiation of **5** (Scheme 4). Complex **6** has been characterised on the basis of mass spectrometry, IR and ^1H and ^{31}P NMR spectroscopy.

The IR spectrum of **6**, in hexane, shows only three bands in the carbonyl region. In the FAB mass spectrum the molecular ion peak (M^+) is seen along with fragment ions due to the loss of $n\text{CO}$ ($n = 1\text{--}3$).

The ^1H NMR spectrum of **6** shows, in addition to signals due to the phenyl, cyclopentadienyl and methylene protons, a hydride signal coupled to three phosphorus nuclei ($^2J(\text{PH})$, 40.1, 40.1 and 16.2 Hz). Again, this is indicative of cis $^2J(\text{PH})$ coupling of the hydride to all



Scheme 4. Formation of W–Mn complexes (**5** and **6**) containing the dppm ligand in chelating and bridging modes.

three phosphorus nuclei. The low-temperature $^{31}\text{P}\{-^1\text{H}\}$ NMR spectrum of **6** exhibits three signals. A downfield resonance ($\delta -51.6$) with ^{183}W satellite peaks ($^1J(\text{WP})$ 171.4 Hz) just discernible is attributed to the $\mu\text{-PPh}_2$ ligand. The other two resonances ($\delta -61.2$ and -112.5) show a large phosphorus–phosphorus coupling ($^2J(\text{PP})$ 133.4 Hz) and are assigned to the two dppm phosphorus nuclei. Such a large $^2J(\text{PP})$ coupling has been observed previously by Stone et al. for dppm ligands bridging WPt in heterobimetallic complexes of these metals [28]. Tungsten satellites ($^1J(\text{WP})$ 178.5 Hz) are observed for the upfield dppm resonance but not for the other dppm resonance, and this is taken as evidence that the dppm ligand adopts a bridging configuration.

It is proposed that the dppm ligand substitutes at the manganese atom in a position cis to both the phosphido and the hydrido bridges (Scheme 4) on the basis of the magnitude of the phosphorus couplings to the hydride and the lack of coupling of the dppm moiety to the phosphido bridge. In the analogous complex $[(\eta^5\text{-C}_5\text{H}_5)(\text{OC})\text{Mo}(\mu\text{-H})(\mu\text{-PPh}_2)(\mu\text{-dppm})\text{Mn}(\text{CO})_3]$, it was proposed that the dppm ligand preferentially substitutes the carbonyl group on manganese that is least sterically hindered by the cyclopentadienyl ligand [5,6]. A major and minor isomer were isolated for this analogous complex which showed three different $^2J(\text{PH})$ values for the bridging hydride signals in each case, the largest being 49.7 Hz and 76.6 Hz respectively. The major isomer was shown by X-ray crystallography to have a structure similar to that illustrated in Fig. 3, whereas the minor isomer was assigned a structure in which the dppm ligand substitutes the other CO group on the Mo atom.

3. Conclusions

For the most part, mono- and bis-substitution of CO groups in **1** by phosphines occurs selectively at the manganese centre. The W–CO group cis to the bridging hydride can, however, be substituted by prolonged photolysis with dppm. In contrast to the results for phosphine substitution, complex **1** can be non-selectively labelled on both metal atoms by thermolysis or photolysis with ^{13}CO .

4. Experimental

All reactions were carried out under a nitrogen atmosphere using standard Schlenk techniques. Solvents were distilled under nitrogen from appropriate drying agents and degassed prior to use. Preparative thin-layer chromatography (TLC) was carried out on commercial Merck plates with a 0.25 mm layer of silica, or on 1 mm silica plates prepared at the University Chemical Labo-

ratory, Cambridge. Column chromatography was performed on Kieselgel 60 (70–230 mesh) or (230–400 mesh). Products are given in order of decreasing R_f values.

The instrumentation used to obtain spectroscopic data has been described previously [5]. Photolysis experiments were conducted in a glass vessel with a quartz inner tube containing a Hanovia medium-pressure UV lamp (125 W). Unless otherwise stated, all reagents were obtained from commercial suppliers and used without further purification.

4.1. Synthesis of $[(\eta^5\text{-C}_5\text{H}_5)(\text{OC})_2\text{W}(\mu\text{-H})(\mu\text{-PPh}_2)\text{Mn}(\text{CO})_4]$ **1**

(a) Firstly, $[(\eta^5\text{-C}_5\text{H}_5)\text{W}(\text{CO})_3(\text{PPh}_2)]$ was synthesised using a slight adaption of the method used by Malisch et al. [8]. The complex $\text{Na}[(\eta^5\text{-C}_5\text{H}_5)\text{W}(\text{CO})_3 \cdot 2\text{DME}]$ (14.97 g, 27.90 mmol) was added to a flask containing toluene (400 ml). Chlorodiphenylphosphine (5.0 ml, 27.90 mmol) was dissolved in toluene (100 ml) and added to the flask *via* a dropping funnel over a period of 0.5 h. The insoluble yellow starting material gradually converted into the red soluble product $[(\eta^5\text{-C}_5\text{H}_5)\text{W}(\text{CO})_3(\text{PPh}_2)]$. The NaCl was filtered off under nitrogen and the solvent was removed under reduced pressure to give $[(\eta^5\text{-C}_5\text{H}_5)\text{W}(\text{CO})_3(\text{PPh}_2)]$.

(b) The anion $[\text{Mn}(\text{CO})_5]^-$ was prepared by stirring $[\text{Mn}_2(\text{CO})_{10}]$ (5.44 g, 13.95 mmol) in a THF (75 ml) solution over Na–K (34.87 mmol) alloy overnight.

(c) The complex $[\text{Mn}(\text{CO})_5]^-$ was added dropwise to a THF (300 ml) solution of $[(\eta^5\text{-C}_5\text{H}_5)\text{W}(\text{CO})_3(\text{PPh}_2)]$ over a period of 0.5 h and then stirred overnight. Addition of H_3PO_4 (88%) (3.1 ml) resulted in a rapid colour change from dark red to orange. The mixture was then stirred for 2 h and filtered. The solvent was removed from the filtrate under reduced pressure and the residue dissolved in the minimum quantity of CH_2Cl_2 and loaded onto the top of a chromatography column. Elution, initially with hexane (100%), gave $[\text{Mn}_2(\text{CO})_{10}]$ (0.93 g, 2.37 mmol); subsequent elution with hexane– CH_2Cl_2 (95:5) gave $[\text{Mn}_2(\mu\text{-H})(\mu\text{-PPh}_2)(\text{CO})_8]$ **2c** (0.40 g, 5.5%) and large amounts of air-sensitive products (not identified). A yellow band was eluted next, which, on subsequent TLC, separated into yellow crystalline $[\text{Mn}_2(\text{CO})_9(\text{PPh}_2\text{H})]$ **2a** (0.45 g, 5.9%) followed by orange-yellow crystalline $[\text{Mn}_2(\text{CO})_9(\text{PPh}_2\text{PPh}_2)]$ **2b** (0.55 g, 5.4%). Orange crystalline $[(\eta^5\text{-C}_5\text{H}_5)(\text{OC})_2\text{W}(\mu\text{-H})(\mu\text{-PPh}_2)\text{Mn}(\text{CO})_4]$ **1** (1.90 g, 10.4%) was eluted next with hexane– CH_2Cl_2 (9:1). Further elution with higher polarity mixtures of hexane– CH_2Cl_2 yielded $[\text{Mn}_2(\mu\text{-PPh}_2)_2(\text{CO})_8]$ **2d** (0.50 g, 5.1%), traces of $[(\eta^5\text{-C}_5\text{H}_5)_2\text{W}_2(\text{CO})_6]$ and $[(\eta^5\text{-C}_5\text{H}_5)_2\text{W}_2(\mu\text{-H})(\mu\text{-PPh}_2)(\text{CO})_4]$ [13] and numerous other unidentified products. Complex **1** (found: C, 42.0; H, 2.8; P, 5.7. $\text{C}_{23}\text{H}_{16}\text{MnO}_6\text{PW}$ requires C, 41.9; H, 2.4; P, 4.7%). EI

mass spectrum: m/e 658 (M^+), $M^+ - n(\text{CO})$ ($n = 1-4$). NMR: ^{13}C (CDCl_3 , 293 K, ^1H gated decoupled), δ 230.9 (s, br, W-CO), 221.7 (s, br, W-CO), 217.8 (s, Mn-CO), 216.5 (s, Mn-CO), 210.0 (br, 2Mn-CO), 140.3 (d, $^1J(\text{PC})$ 38, P-C), 133.6 (d, $^2J(\text{PC})$ 7, *o*-Ph), 129.2 (s, *p*-Ph), 128.2 (d, $^3J(\text{PC})$ 10, *m*-Ph) and 89.9 (s, Cp); ^{13}C (CDCl_3 , 225 K, ^1H gated decoupled), 232.3 (d, $^2J(\text{PC})$ 21, 1W-CO(*cis*)), 222.0 (s, 1W-CO(*trans*)), 217.8 (s, Mn-CO), 216.5 (s, Mn-CO), 211.5 (d, $^2J(\text{PC})$ 13, MnCO), 208.1 (d, $^2J(\text{PC})$ 14, MnCO), 139.3 (d, $^1J(\text{PC})$ 29, P-C), 138.7 (d, $^1J(\text{PC})$ 29.7, P-C), 134.6 (d, $^2J(\text{PC})$ 8.9, *o*-Ph), 131.9 (d, $^2J(\text{PC})$ 11, *o*-Ph), 129.8 (s, *p*-Ph), 128.6 (d, $^3J(\text{PC})$ 10, *m*-Ph), 128.5 (s, *p*-Ph), 127.8 (d, $^3J(\text{PC})$ 11, *m*-Ph) and 89.9 (s, Cp). Complex **2b** (found: C, 54.6; H, 3.0; P, 8.3. $\text{C}_{33}\text{H}_{20}\text{Mn}_2\text{O}_9\text{P}_2$ requires C, 54.1; H, 2.7; P, 8.5%). EI mass spectrum: m/e 676 ($M^+ - 2\text{CO}$). NMR: ^{13}C (CD_2Cl_2 , 220 K, ^1H gated decoupled), δ 222.9 (d, $J(\text{PC})$ 12, CO) and 140–128 (m, Ph).

4.2. Substitution reactions of complex $[(\eta^5\text{-C}_5\text{H}_5)(\text{OC})_2\text{W}(\mu\text{-H})(\mu\text{-PPh}_2)\text{Mn}(\text{CO})_4] \mathbf{1}$

4.2.1. With ^{13}CO

Complex **1** (0.170 g, 0.26 mmol) was dissolved in toluene (150 ml). The solution was then put through three cycles of freezing, degassing and thawing before excess ^{13}CO was condensed into the apparatus, which was then sealed. The solution was heated at 333 K for 48 h after which time the solvent was removed under reduced pressure and the product purified through a Celite plug.

4.2.2. With $\text{P}(\text{OMe})_3$

Complex **1** (0.110 g, 0.17 mmol) and $\text{P}(\text{OMe})_3$ (0.039 ml, 0.34 mmol) were dissolved in a hexane-toluene mixture (130 ml:40 ml) and the solution was irradiated with UV light for 100 min to give a cloudy orange-red solution. The solvent was removed under reduced pressure and the residue dissolved in the minimum quantity of CH_2Cl_2 and applied to the base of TLC plates. Elution with hexane- CH_2Cl_2 (4:1) gave **1** (0.002 g) followed by orange crystalline $[(\eta^5\text{-C}_5\text{H}_5)(\text{OC})_2\text{W}(\mu\text{-H})(\mu\text{-PPh}_2)\text{Mn}(\text{CO})_3\{\text{P}(\text{OMe})_3\}] \mathbf{3a}$ (0.030 g, 24%) and orange-red crystalline $[(\eta^5\text{-C}_5\text{H}_5)(\text{OC})_2\text{W}(\mu\text{-H})(\mu\text{-PPh}_2)\text{Mn}(\text{CO})_2\{\text{P}(\text{OMe})_3\}_2] \mathbf{4a}$ (0.075 g, 53%). The yield of **3a** relative to **4a** was increased by the use of equimolar amounts of **1** and $\text{P}(\text{OMe})_3$. Complex **3a**: EI mass spectrum: m/e 754 (M^+), $M^+ - n(\text{CO})$ ($n = 0, 3, 4$). NMR: ^{13}C (CDCl_3 , 240 K, ^1H gated decoupled), δ 233.3 (s, br, W-CO(*cis*)), 224.9 (s, WCO(*trans*)), 220.8 (m, MnCO), 213.5 (m, MnCO), 208.5 (m, MnCO), 141–127 (m, Ph), 89.6 (s, Cp) and 52.1 (s, OMe). Complex **4a** (found: C, 37.2; H, 4.0; P, 10.7. $\text{C}_{27}\text{H}_{34}\text{MnO}_{10}\text{P}_3\text{W}$ requires C, 38.1; H, 4.0; P, 10.9%). EI mass spectrum:

m/e 850 (M^+), $M^+ - n(\text{CO})$ ($n = 1-3$). NMR: ^{13}C (CDCl_3 , 250 K, ^1H gated decoupled), δ 237.1 (d, $^2J(\text{PC})$ 10, WCO(*cis*)), 227.9 (s, W-CO(*trans*)), 217.9 (m, MnCO), 215.7 (m, MnCO), 144.5 (d, $^1J(\text{PC})$ 31, P-C), 142.2 (d, $^1J(\text{PC})$ 33, P-C), 134.9 (d, $^2J(\text{PC}) < 5$, *o*-Ph), 133.0 (d, $^2J(\text{PC})$ 8, *o*-Ph), 128.2 (s, *p*-Ph), 127.7 (s, *m*-Ph), 126.9 (s, *p*-Ph), 126.9 (obscured, *m*-Ph), 89.9 (s, Cp) and 52.0 (s, br, OMe).

4.2.3. With PMe_2Ph

Complex **1** (0.110 g, 0.17 mmol) and PMe_2Ph (0.048 ml, 0.34 mmol) were used as in Section 4.2.2, though irradiation time was increased to 3 h, to give **1** (0.020 g), orange crystalline $[(\eta^5\text{-C}_5\text{H}_5)(\text{OC})_2\text{W}(\mu\text{-H})(\mu\text{-PPh}_2)\text{Mn}(\text{CO})_3(\text{PMe}_2\text{Ph})] \mathbf{3b}$ (0.061 g, 48%) and red crystalline $[(\eta^5\text{-C}_5\text{H}_5)(\text{OC})_2\text{W}(\mu\text{-H})(\mu\text{-PPh}_2)\text{Mn}(\text{CO})_2(\text{PMe}_2\text{Ph})_2] \mathbf{4b}$ (0.024 g, 16%). Complex **3b**: EI mass spectrum: m/e 768 (M^+), $M^+ - n(\text{CO})$ ($n = 1-3$). Complex **4b** (found: C, 50.2; H, 4.3. $\text{C}_{37}\text{H}_{38}\text{MnO}_4\text{P}_3\text{W}$ requires C, 50.6; H, 4.3%). Fast atom bombardment (FAB) mass spectrum: m/e 878 (M^+).

4.2.4. With PMePh_2

Complex **1** (0.110 g, 0.17 mmol) and PMePh_2 (0.06 ml, 0.32 mmol) were used as in Section 4.2.2 to give **1** (0.010 g), orange crystalline $[(\eta^5\text{-C}_5\text{H}_5)(\text{OC})_2\text{W}(\mu\text{-H})(\mu\text{-PPh}_2)\text{Mn}(\text{CO})_3(\text{PMePh}_2)] \mathbf{3c}$ (0.073 g, 53%) and trace amounts of a red uncharacterised product, presumably the disubstituted derivative. Complex **3c** (found: C, 50.6; H, 3.4; P, 6.9. $\text{C}_{35}\text{H}_{29}\text{MnO}_5\text{P}_2\text{W}$ requires C, 50.6; H, 3.5; P, 7.5%). EI mass spectrum: m/e 830 (M^+), $M^+ - n(\text{CO})$ ($n = 1$).

4.2.5. With PPh_2H

Complex **1** (0.100 g, 0.15 mmol) and PPh_2H (0.026 ml, 0.15 mmol) were dissolved in toluene (50 ml) and the solution heated initially to 333 K for 1.5 h and then to 348 K for a further 2.5 h. The solvent was removed under reduced pressure and the residue dissolved in the minimum quantity of CH_2Cl_2 and applied to TLC plates. Elution with hexane- CH_2Cl_2 (9:1) gave yellow-orange $[(\eta^5\text{-C}_5\text{H}_5)(\text{OC})_2\text{W}(\mu\text{-H})(\mu\text{-PPh}_2)\text{Mn}(\text{CO})_3(\text{PPh}_2\text{H})] \mathbf{3d}$ (0.086 g, 69%) as the only product. Complex **3d**: EI mass spectrum: m/e 734 ($M^+ - 816$). NMR: ^{13}C (CDCl_3 , 293 K, ^1H gated decoupled), δ 224.3 (m, CO), 216.5 (m, CO), 142–127 (m, Ph) and 89.3 (s, Cp).

4.2.6. With dppm

Complex **1** (0.050 g, 0.08 mmol) and dppm (0.058 g, 0.15 mmol) were used as in Section 4.2.2, photolysis time being 6.5 h, to give orange crystalline $[(\eta^5\text{-C}_5\text{H}_5)(\text{OC})_2\text{W}(\mu\text{-H})(\mu\text{-PPh}_2)\text{Mn}(\text{CO})_2(\text{dppm})] \mathbf{5}$ (0.051 g, 68%) and red-purple, slightly air-sensitive, $[(\eta^5\text{-C}_5\text{H}_5)(\text{OC})\text{W}(\mu\text{-H})(\mu\text{-PPh}_2)(\mu\text{-dppm})\text{Mn}(\text{CO})_3]$

6 (0.011 g, 15%). Complex **5** (found: C, 55.9; H, 3.9; P, 9.2. $C_{46}H_{38}MnO_4P_3W$ requires C, 56.0; H, 3.9; P, 9.4%). FAB mass spectrum: m/e 986 (M^+), $M^+ - n(CO)$ ($n = 1-2$). NMR: ^{13}C (CD_2Cl_2 , 230 K, 1H gated decoupled), δ 237.7 (d, $^2J(PC)$ 17, WCO(*cis*)), 229.9 (s, WCO(*trans*)), 227.5 (m, MnCO), 225.3 (m, MnCO), 146–126 (m, Ph), 90.6 (s, Cp) and 49.7 (m, $PPh_2CH_2PPh_2$). Complex **6**: FAB mass spectrum: m/e 986 (M^+), $M^+ - n(CO)$ ($n = 1-3$).

4.3. Reactions of phosphine adducts of **1**

4.3.1. Attempt to convert $[(\eta^5-C_5H_5)(OC)_2W(\mu-H)(\mu-PPh_2)Mn(CO)_3(PPh_2H)]$ **3d** to a bis-phosphido compound

Complex $[(\eta^5-C_5H_5)(OC)_2W(\mu-H)(\mu-PPh_2)Mn(CO)_3(PPh_2H)]$ **3d** (0.035 g, 0.04 mmol) was dissolved in toluene (50 ml) and the solution heated to 358 K whilst the reaction was monitored both by spot TLC and IR spectroscopy. The solution was maintained at this temperature for 4 h during which time steady decomposition occurred, compound **3d** being the only recoverable product.

4.3.2. Photolysis of $[(\eta^5-C_5H_5)(OC)_2W(\mu-H)(\mu-PPh_2)Mn(CO)_2(dppm)]$ **5**

Complex $[(\eta^5-C_5H_5)(OC)_2W(\mu-H)(\mu-PPh_2)Mn(CO)_2(dppm)]$ **5** (0.071 g, 0.07 mmol) was dissolved in toluene (150 ml) and irradiated with UV light overnight to give unreacted **5** (0.015 g), an unidentified orange band in low yield, $[(\eta^5-C_5H_5)(OC)W(\mu-H)(\mu-PPh_2)(\mu-dppm)Mn(CO)_3]$ **6** (0.010 g, 14%) and significant amounts of decomposition.

4.4. X-ray crystal structure determination of **1**

Suitable crystals of $[(\eta^5-C_5H_5)(OC)_2W(\mu-H)(\mu-PPh_2)Mn(CO)_4]$ **1** were grown from a dichloromethane solution by slow diffusion of hexane at 273 K. A single crystal was mounted on a goniometer head using epoxy resin and transferred to a Stoe four-circle diffractometer.

Crystal data. $C_{23}H_{16}MnO_6PW$, $M = 658.14$, monoclinic $C2/c$, $a = 27.863(12)$, $b = 14.191(10)$, $c = 14.249(6)$ Å, $\beta = 105.83(3)^\circ$, $U = 5420.43$ Å³, $Z = 8$, $D_c = 1.54$ g cm⁻³, $F(000) = 2528$, $\mu(Mo K\alpha) = 45.6$ cm⁻¹.

An orange needle-shaped crystal with approximate dimensions $0.40 \times 0.18 \times 0.14$ mm was used. Accurate cell dimensions were obtained from 50 reflections in the range $18 \leq 2\theta \leq 25^\circ$. Intensity data were recorded using graphite-monochromated Mo K α radiation ($\lambda = 0.71069$ Å), and an ω - θ scan mode to a maximum 2θ value of 45° . Three standard reflections were monitored hourly throughout the data collection and showed no significant variation in intensity.

A total of 7783 intensities were measured within the range $-30 \leq h \leq 30$, $-15 \leq k \leq 0$, $0 \leq l \leq 15$ and averaged to give 3544 unique reflections ($R_{int} = 0.0596$) of which 2699 were judged as significant using the criterion $F_{obs} > 4\sigma(F_{obs})$. Corrections for Lorentz and polarisation effects were applied. A numerical absorption correction based on a crystal bounded by the planes $\{100\}$, $\{\bar{1}10\}$, $\{11\bar{1}\}$ and $\{111\}$ was applied; min. and max. transmission, 0.570, 0.375. The structure was solved by a combination of Patterson methods and Fourier difference techniques. The structure was refined by full-matrix least squares with all non-hydrogen atoms assigned anisotropic displacement parameters [29]. Hydrogen atoms were placed in idealised positions and allowed to ride on the relevant carbon atom with C–H = 0.96 Å; hydrogen atoms were refined with a common displacement parameter of 0.11 Å². In the final cycles of refinement a weighting scheme of the form $w = 2.0923/[\sigma^2(F) + 0.00013F^2]$ which gave satisfactory agreement analysis was introduced. The refinement converged to $R = 0.0636$ and $R_w = 0.0611$. Residual electron-density peaks in final difference map, max. 2.38 e Å⁻³, min. -1.45 e Å⁻³. Final atomic coordinates are listed in Table 3.

Additional crystallographic data including hydrogen-atom coordinates, displacement parameters and full lists of bond parameters have been deposited with the Cambridge Crystallographic Data Centre. Lists of structure factors are available from the authors.

Acknowledgements

We thank the EPSRC (S.M.O., P.F.R., G.P.S. and G.A.S.) for financial support.

References

- [1] (a) M.I. Bruce, *J. Organomet. Chem.*, 283 (1985) 339. (b) G. L. eoffroy, *Acc. Chem. Res.*, 13 (1980) 469. (c) J. Powell, M.R. Gregg and J.F. Sawyer, *J. Chem. Soc. Chem. Commun.*, (1983) 1149. (d) J. Powell, J.F. Sawyer and M.V.R. Stainer, *J. Chem. Soc. Chem. Commun.*, (1985) 1314. (e) H. Lehner, A. Musco, L.M. Venanzi and A. Albinati, *J. Organomet. Chem.*, 213 (1981) C46. (f) J. Powell, J.F. Sawyer and S.J. Smith, *J. Chem. Soc. Chem. Commun.*, (1985) 1312. (g) P.A. Tooley, L.W. Arndt and M.Y. Darensbourg, *J. Am. Chem. Soc.*, 107 (1985) 2422.
- [2] A.D. Horton, M.J. Mays and P.R. Raithby, *J. Chem. Soc. Chem. Commun.*, (1985) 247.
- [3] (a) P.M. Treichel, W.K. Dean and W.M. Douglas, *Inorg. Chem.*, 11 (1972) 1609. (b) R.B. King, W.-K. Fu and E.M. Holt, *J. Chem. Soc. Chem. Commun.*, (1984) 1439. (c) B.E. Hanson, P.E. Fanwick and J.S. Mancini, *Inorg. Chem.*, 21 (1982) 3811. (d) E.P. Kyba, J.D. Mather, K.L. Hassett, J.S. McKennis and R.E. Davis, *J. Am. Chem. Soc.*, 106 (1984) 5371.
- [4] J.A. Iggo, M.J. Mays, P.R. Raithby and K. Henrick, *J. Chem. Soc. Dalton Trans.*, (1983) 205.

- [5] A.J.M. Caffyn, M.J. Mays and P.R. Raithby, *J. Chem. Soc. Dalton Trans.*, (1991) 2349.
- [6] A.D. Horton, M.J. Mays and P.R. Raithby, *J. Chem. Soc. Dalton Trans.*, (1987) 1557.
- [7] R.P. Rosen, J.B. Hoke, R.R. Whittle, G.L. Geoffroy, J.P. Hutchinson and J.A. Zubieta, *Organometallics*, 3 (1984) 846.
- [8] W. Malisch, R. Maisch, I.J. Colquhoun and W. McFarlane, *J. Organomet. Chem.*, 220 (1981) C1.
- [9] J.E. Ellis and E.A. Flom, *J. Organomet. Chem.*, 99 (1975) 263.
- [10] R. Giordano, E. Sappa, A. Tiripicchio, M. Tiripicchio Camellini, M.J. Mays and M.P. Brown, *Polyhedron*, 8 (1989) 1855.
- [11] J.A. Iggo, M.J. Mays, P.R. Raithby and K. Henrick, *J. Chem. Soc. Dalton Trans.*, (1984) 633.
- [12] M.L.H. Green and J.T. Moelwyn-Hughes, *Z. Naturforsch. Teil B.*, 17 (1962) 783. L. Manojlovic-Muir, M.J. Mays, K.W. Muir and K.W. Woulfe, *J. Chem. Soc. Dalton Trans.*, (1992) 1531.
- [13] M.J. Mays, unpublished results
- [14] A.D. Horton, A.C. Kembal and M.J. Mays, *J. Chem. Soc. Dalton Trans.*, (1988) 2953.
- [15] P. Legzdins, J.T. Martin, F.W.B. Einstein and A.C. Willis, *J. Am. Chem. Soc.*, 108 (1986) 7971.
- [16] S.-G. Shyu, J.-Y. Hsu, P.-J. Lin, W.-J. Wu, S.-M. Peng, G.-F. Lee and Y.-S. Wen, *Organometallics*, 13 (1994) 1699.
- [17] L.J. Todd, J.R. Wilkinson, J.P. Hickey, D.L. Beach and K.W. Barnett, *J. Organomet. Chem.*, 154 (1978) 151.
- [18] C.P. Casey and R.M. Bullock, *J. Organomet. Chem.*, 218 (1981) C47.
- [19] K. Henrick, M. McPartlin, A.D. Horton and M.J. Mays, *J. Chem. Soc. Dalton Trans.*, (1988) 1083.
- [20] J.L. Petersen, L.F. Dahl and J.A. Williams, *J. Am. Chem. Soc.*, 96 (1974) 6610.
- [21] Yu.T. Struchkov, K.N. Anisimov, O.P. Osipova, N.E. Kolobova and A.N. Nesmeyanov, *Proc. Acad. Sci. USSR*, 172 (1967) 15.
- [22] N.E. Kolobova, L.L. Ivanov, O.S. Zhvanko, A.S. Batsanov and Yu.T. Struchkov, *J. Organomet. Chem.*, 279 (1985) 419.
- [23] I.J. Hart, J.C. Jeffery, R.M. Lowry and F.G.A. Stone, *Angew. Chem. Int. Ed. Engl.*, 27 (1988) 1703.
- [24] E. Fluck and K. Issleib, *Chem. Ber.*, 98 (1965) 2674.
- [25] G. Wilkinson, F.G.A. Stone and E.W. Abel (eds.), *Comprehensive Organometallic Chemistry*, Pergamon, Oxford, Chapter 29, p. 4. M. Laing, E. Singleton and R. Reimann, *J. Organomet. Chem.*, 56 (1973) C21. E.O. Fischer and W.A. Herrmann, *Chem. Ber.*, 105 (1972) 286. M. Ziegler, H. Haas and R.K. Sheline, *Chem. Ber.*, 98 (1965) 2454.
- [26] J. Ellermann and H.A. Lindner, *Z. Naturforsch. Teil B.*, 34 (1979) 799. R.H. Reimann and E. Singleton, *J. Chem. Soc. Dalton Trans.*, (1976) 2109.
- [27] G.A. Carriedo, V. Riera and J. Santamaria, *J. Organomet. Chem.*, 234 (1982) 175.
- [28] K.A. Mead, I. Moore, F.G.A. Stone and P. Woodward, *J. Chem. Soc. Dalton Trans.*, (1983) 2083.
- [29] G.M. Sheldrick, SHELX-76, *A Program for Crystal Structure Determination*, University of Cambridge, 1976.